

Unsupervised semantic and instance segmentation of forest point clouds

Di Wang

Department of Built Environment, Aalto University, P.O. Box 14100, Aalto 00076, Finland



ARTICLE INFO

Keywords:

Terrestrial LiDAR
Tree isolation
Component classification
Segmentation
Superpoint graph

ABSTRACT

Terrestrial Laser Scanning (TLS) has been increasingly used in forestry applications including forest inventory and plant ecology. Tree biophysical properties such as leaf area distributions and wood volumes can be accurately estimated from TLS point clouds. In these applications, a prerequisite is to properly understand the information content of large scale point clouds (i.e., semantic labelling of point clouds), so that tree-scale attributes can be retrieved. Currently, this requirement is undergoing laborious and time consuming manual works. In this work, we jointly address the problems of semantic and instance segmentation of forest point clouds. Specifically, we propose an unsupervised pipeline based on a structure called superpoint graph, to simultaneously perform two tasks: single tree isolation and leaf-wood classification. The proposed method is free from restricted assumptions of forest types. Validation using simulated data resulted in a mean Intersection over Union (mIoU) of 0.81 for single tree isolation, and an overall accuracy of 87.7% for leaf-wood classification. The single tree isolation led to a relative root mean square error (RMSE%) of 2.9% and 19.8% for tree height and crown diameter estimations, respectively. Comparisons with existing methods on other benchmark datasets showed state-of-the-art results of our method on both single tree isolation and leaf-wood classification tasks. We provide the entire framework as an open-source tool with an end-user interface. This study closes the gap for using TLS point clouds to quantify tree-scale properties in large areas, where automatic interpretation of the information content of TLS point clouds remains a crucial challenge.

1. Introduction

The advancements of Light Detection and Ranging (LiDAR) technique have revolutionized tree structural quantification in past years (Dassot et al., 2011). The unique advantage of LiDAR technique is that it acquires detailed three dimensional (3D) representations (i.e., point clouds) of objects. Ground-based LiDAR, or Terrestrial Laser Scanning (TLS), is the technique that by far provides the most accurate measures at the scale of individual trees (Liang et al., 2016). Comparing to conventional forest inventories and destructive measurements, TLS is able to rapidly and automatically document tree structures with millimeter-level details. Alongside the highly accurate 3D coordinates, TLS is also able to provide radiometric properties of objects, thus holds great potentials for vegetation studies (Kaasalainen et al., 2009).

The applications of TLS in forestry can be broadly grouped into two fields, forest inventory and plant ecology. In forest inventory, the attention is paid on tree stems. Attributes such as stem position, diameter at the breast height (DBH), and stem curve can be accurately estimated with TLS point clouds (Liang et al., 2018). On the other hand, plant ecology focuses on using TLS to estimate tree physiological properties such as leaf angle distribution (Liu et al., 2019), gap fraction (Danson

et al., 2007), canopy radiation (Van Leeuwen et al., 2013), and above-ground biomass (AGB) (Calders et al., 2015).

However, most of these applications require the TLS point clouds to be properly interpreted in advance (e.g., filtered, segmented, classified) (Morsdorf et al., 2018). This requirement is particularly vital for plant ecology studies, as the focus is often on different material components at the scale of individual trees. For example, the estimation of tree AGB is primarily done using the so-called quantitative structure models (QSM) that reconstruct the 3D woody structure of individual trees (Gonzalez de Tanago et al., 2018; Takoudjou et al., 2018). An accurate QSM reconstruction relies on a well filtered point cloud of single tree woody components (Calders et al., 2015). In addition, woody materials have to be removed for understanding the canopy radiation regime and photosynthetic processes. Moreover, new application opportunities such as mass and energy exchange will emerge if TLS point clouds can be properly filtered and processed. Therefore, it is important to interpret the information content of TLS point clouds in advance for forest applications (Morsdorf et al., 2018; Burt et al., 2019).

The interpretation of the information content (i.e., semantic labelling) of forest point clouds mainly involves three processes: terrain removal, single tree isolation, and components (i.e., leaf-wood)

E-mail address: di.wang@aalto.fi.

classification. Terrain filtering in forested areas is one of the early applications of LiDAR techniques, and has been extensively studied (Puttonen et al., 2014). However, less advancements were achieved on single tree isolation and leaf-wood classification. These two processes can be further categorized into two general point cloud processing problems: semantic segmentation and instance segmentation. Specifically, leaf-wood classification belongs to the problem of semantic segmentation, where the goal is to associate each point with a class label (i.e., leaf or wood) (Tchapmi et al., 2017). Single tree isolation is with the topic of instance segmentation, a process that clusters the scene into object instances (i.e., individual trees). So far, both processes have been undergone laborious and time consuming manual works. Recently, several approaches were developed to tackle these issues respectively (e.g., Burt et al., 2019; Heinzel and Huber, 2018; Wang et al., 2018; Vicari et al., 2019; Wang et al., 2020). However, several obstacles still remain. First, manual delineation and correction in point clouds are still often required. Second, single tree isolation methods have not yet been properly evaluated, due to the lack of references on individual tree crowns. Third, previous methods treated single tree isolation and leaf-wood classification as two separate tasks. The potential and advantage of combining semantic and instance segmentation remain unexplored for forest scenes. Lastly, the robustness of previous methods, especially when combined, are unknown for structurally complex forest plots.

In this study, we propose a fully unsupervised approach that simultaneously addresses the tasks of semantic and instance segmentation of forest point clouds. Specifically, this novel method is based on a superpoint graph that enables us to design a series of graph operators to link single tree isolation and leaf-wood classification in a joint optimization routine. Particularly, the intuition was that these two steps can complement each other. The main contributions are as follows:

- A novel superpoint graph representation of the original forest point cloud that is embedded with rich node and edge features encoding the contextual information at the object level.
- An unsupervised dual-task network architecture operating on the superpoint graph that simultaneously performs two tasks: single tree isolation and leaf-wood classification.
- A synthetic TLS dataset simulated on a highly realistic forest scene crafted with more than 20 million triangle meshes. The scene contains large trees with structurally complex crowns. This unique dataset, for the first time, allows the explicit assessment of single tree isolation on tree crowns.
- Experiments on the simulated and other benchmark datasets to validate the effectiveness of the proposed method. Results showed that the concerted semantic and instance segmentation achieved state-of-the-art performance on each individual tasks.

This paper is organized as follows. An overview of related works is given in Section 2. In Section 3, we introduce the synthetic dataset and other benchmark datasets. The detailed description of the proposed method is given in Section 4. Experiment results are presented in Section 5. Afterwards, Section 6 discusses the advantages of the proposed method and challenges in semantic and instance segmentation of forest point clouds. The paper is finally concluded in Section 7.

2. Related work

2.1. Single tree isolation

Single tree isolation in TLS point clouds generally involves two sub-tasks: single tree locating and crown segmentation. The first part refers to the detection of tree stems, and is the central requirement of forest inventory. Various methods have been proposed, such as Euclidean clustering (Hackenberg et al., 2015), circle/cylinder detection (Burt et al., 2019), and 2D point cloud projection (Wang et al., 2016). The recent international benchmarking of TLS methods for forestry

applications extensively evaluated and compared various algorithms from 18 participants (Liang et al., 2018). Overall, stem detection is a well studied topic.

However, on the other hand, crown segmentation using TLS data received much less attention (Heinzel and Huber, 2018). Barbeito et al. (2017) used a k-nearest neighbor algorithm with the assist of marked tapes on the trees in the field. Wang et al. (2019) deployed the Faster R-CNN deep learning network based on projected images to locate tree stems. Then tree crowns were segmented using a region growing method. Raumonen et al. (2015) proposed a morphological rule based approach. Tree stems were located first, and were expanded based on fixed distance connectivity assumptions step by step. Similar idea was used in Trochta et al. (2017). The drawback of this method is that it only works for open forests, where trees are sparse and have minimal interaction between crowns (Burt et al., 2019). A different group of methods used graph theory. These methods intrinsically transformed the point cloud to a connected graph. For example, Zhong et al. (2016) employed normalized graph cut as an energy minimization technique to cluster crown points to candidate stems. Similarly, Yang et al. (2016) hierarchically segmented crowns using minimum graph cut. Heinzel and Huber (2018) developed a constrained spectral clustering approach that minimized the energy of a Markov Random Field. Tao et al. (2015) further introduced ecological theory via metabolic scaling theory (West et al., 1997), which was based on the graph shortest path algorithm. Their method was able to segment intersected crowns. Although different clustering approaches were used, all above-mentioned methods were in fact came to a consensus that tree crowns should be spatially close to the respective stems/roots, an assumption that is obviously inspired by ecological and botanic rules.

In addition to the methodology developments, the assessment of single tree isolation remains an unsolved problem. The challenge is that references on tree crowns are extremely difficult to obtain, even visually in a point cloud. Almost all previous methods, except Heinzel and Huber (2018), evaluated their methods on tree locations only. Heinzel and Huber (2018) additionally manually delineated crown outlines, and compared the 3D volumes of segmented crowns with manual delineation. However, the assessment of point-wise crown segmentation has yet been materialized.

2.2. Leaf-wood classification

A number of approaches have been proposed to classify tree leaf and wood components in a TLS point cloud. Based on the used features, these methods can be grouped into three categories: geometry based, intensity based, and the combination of both (e.g., Wang et al., 2018; Vicari et al., 2019; Krishna Moorthy et al., 2019).

Geometry based methods required only the 3D coordinates of points. A common strategy was to deploy supervised machine learning classifiers. Geometric features, which were usually inferred from the spatial arrangement of neighboring points, were learned for each point. The selection of neighborhoods was either based on fixed or adaptive sizes (Wang et al., 2018; Krishna Moorthy et al., 2019). The determination of features was crucial. Informative and discriminating features should be designed. Studies have shown that machine learning based approaches using only geometric features were able to effectively discriminate leaf and wood points (e.g., Belton et al., 2013; Ma et al., 2015; Yun et al., 2016; Krishna Moorthy et al., 2019). The achieved classification accuracy generally ranged from 80% to 95%. The advantages of these methods are being free from restricted forest types and data sources (Disney et al., 2018). However, the drawback is obvious. Supervise machine learning approaches require laborious and time consuming manual selection of training data. Currently, no large annotated datasets are available for forest scenes. The potential of designing a universal deep learning network for leaf-wood classification remains unexplored. Therefore, it is likely that manual selection of training data is required for each specific dataset, which prevents the

applicability of these approaches for large spatial datasets. A different and preferable strategy of geometry based methods is to develop fully unsupervised approaches. Several automatic algorithms were proposed recently (e.g., Tao et al., 2015; Hétroy-Wheeler et al., 2016; Li et al., 2017; Wang et al., 2018; Vicari et al., 2019; Wang et al., 2020). These unsupervised methods used clustering strategies based on specific geometric properties of components, such as flat leaves, linear structures and circle-like shapes of stems and branches. It is noted that several of these methods were optimized for single trees only (e.g., Tao et al., 2015; Vicari et al., 2019). Additional steps were needed in advance to segment individual trees. Experiments showed that these unsupervised methods achieved similar accuracies compared to supervised machine learning approaches, thus hold great potentials for large-area applications.

On the other hand, intensity based methods assumed that tree components have different optical properties at the operating wavelength of the laser scanner (Béland et al., 2014; Tao et al., 2015). Previous studies have shown that the effectiveness of intensity based methods were similar to geometry based ones (Wang et al., 2018). However, one of the main limitations of intensity based methods is that laser return intensity can be arbitrarily influenced by the distance, a partial laser hit and the incidence angle (Kaasalainen et al., 2009), and has to be calibrated specifically to each instrument (Calders et al., 2017). If calibrated, intensity information can be integrated with geometric features in those geometry based methods, which may provide additional advantages over using only one type (Zhu et al., 2018). Moreover, research-led developments of multi-wavelength LiDAR systems can potentially help to differentiate leaf and wood components in the future (Disney, 2019).

3. Study data

The assessments of both single tree isolation and leaf-wood classification tasks require exhaustive reference data that are usually generated by manual works. However, isolation of single tree crowns in a point cloud is even visually impractical. To mitigate this issue, we designed a unique synthetic dataset with 100% certain point-wise tree IDs and leaf-wood labels. In addition, two other benchmark datasets were used to further compare our method with literature. It is noted that we operate on point clouds normalized by terrains (i.e., with height above ground). Terrain filtering is out of the focus of this study. See e.g., Puttonen et al. (2014) and Moudry et al. (2020) for a concrete description and discussion of terrain filtering in forested regions.

3.1. Synthetic dataset

In this study, 10 base models of European Beech (*Fagus sylvatica*) were firstly modeled using the SpeedTree software (Interactive Data Visualization, Inc. Lexington, SC, USA). For all trees, each leaf was shaped by a diamond (i.e., two triangles), to be consistent with other simulation studies (Gastellu-Etchegorry et al., 2015; Liu et al., 2019). Each tree was duplicated twice. In total, 30 trees were generated in this study to assemble a virtual plot. Specifically, all 30 trees were randomly placed, scaled, and rotated in a $\sim 40 \times 40$ m plot (Fig. 1). This virtual scene consisted of more than 20 million triangle mesh models. Statistics on tree height, DBH, and crown diameter are summarized in Fig. 2. We intentionally created large and significantly intersected crowns, to fully validate the effectiveness of our method.

TLS point clouds were simulated using the HELIOS simulator (Bechtold and Höfle, 2016). HELIOS is an open-source tool that allows users to simulate various laser scanning platforms on virtual scenes assembled by mesh models. In this study, we simulated the setting and specifications of Riegl VZ-400 (0.3 mrad beam divergence, 0.05° angular resolution), a popular scanner used in forestry studies. Scans from nine locations were simulated, with four outside, four at the corners and one at the center (Fig. 3). This setting was to ensure a high point cloud quality (Wilkes et al., 2017), as this scene is characterized with large and structurally complex crowns that will lead to heavy occlusions. Prior information of tree IDs and leaf-wood labels were recorded in TLS simulation. The simulated point clouds from nine locations were merged. The final point cloud was downsampled by 1 cm voxels to reduce the data size. Each resulting point contained an ID for tree marking and a label indicating the leaf and wood class.

3.2. Benchmark datasets

Two additional benchmark datasets were included in this study to compare our method with others in literature on single tree isolation and leaf-wood classification, respectively.

3.2.1. Single tree isolation

Openly available TLS datasets of six forest plots were obtained from the international TLS benchmarking project organized by the Finnish Geospatial Research Institute (Liang et al., 2018). These datasets were acquired from southern boreal forests in Evo, Finland, covering various tree species, stem densities, developing stages, and abundance of understorey vegetation. According to these characteristics, six plots were categorized into three complexity types (i.e., easy, medium, and

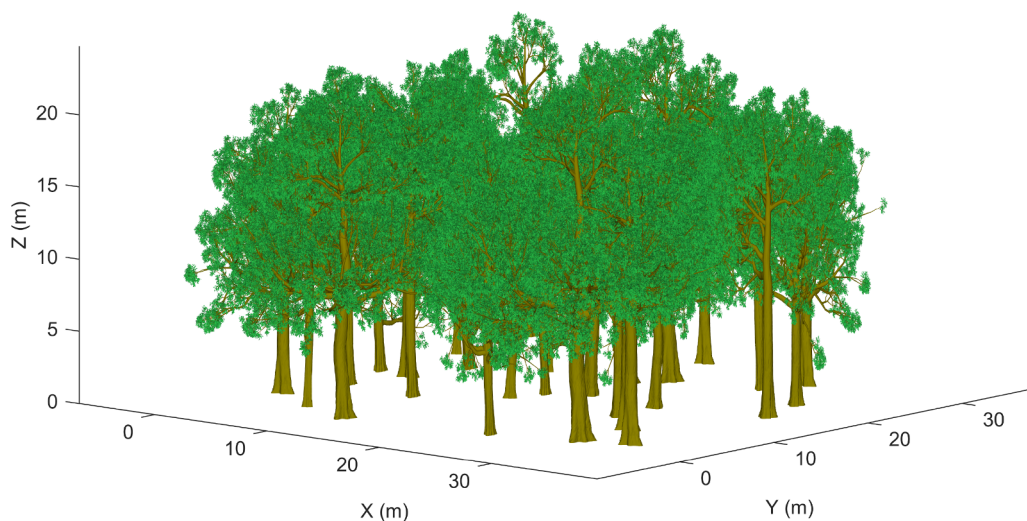


Fig. 1. A 40×40 m virtual forest plot.

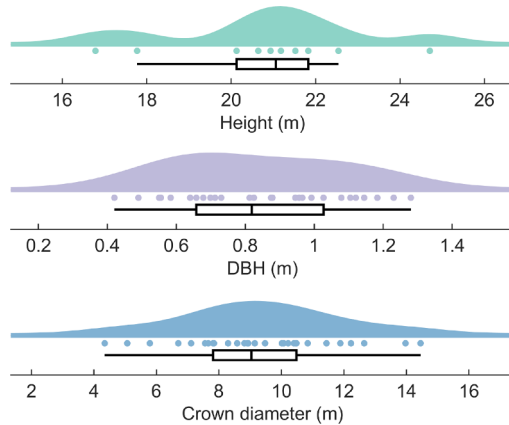


Fig. 2. Distributions of tree attributes. The box plots show the the minimum, first quartile, median, third quartile, and maximum values. (For interpretation of the references to colour in this figure legend, the reader is referred to the web version of this article.)

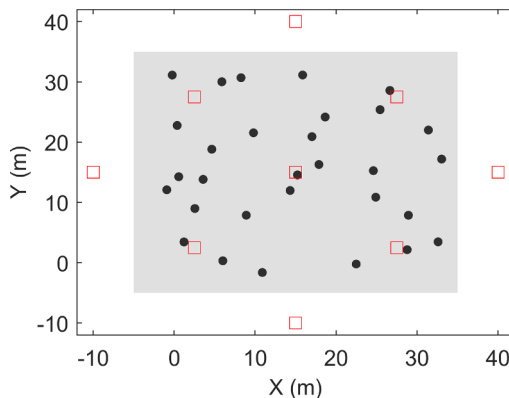


Fig. 3. Tree (black dots) and TLS scan (red squares) positions. The 40×40 m plot is colored by gray. (For interpretation of the references to colour in this figure legend, the reader is referred to the web version of this article.)

difficult). The dominant tree species were Scots pine (*Pinus sylvestris* L.), Norway spruce (*Picea abies* L. Karst.), silver birch (*Betula pendula* Roth), and downy birch (*Betula pubescens* Ehrh.). Each plot had a fixed size of 32×32 m, and was scanned by the Leica HDS1600 scanner (Leica Geosystems AG, Heerbrugg, Switzerland). Both single- and multi-scan data were provided. Only multi-scan data were used in this study, as we focus on detailed crown segmentation. Reference data of tree positions and DBHs were provided. Terrain points were filtered by using the open-source cloth simulation method (Zhang et al., 2016). See Liang et al. (2018) for a full description of the benchmark plots used in this study.

3.2.2. Leaf-wood classification

A forest plot with 50 m radius in Großgöttfritz, the federal state of Lower Austria (Austria) was used in this study as a benchmark dataset for leaf-wood classification. The dominant tree species was Scots pine (*Pinus sylvestris* L.), with a couple of silver birch (*Betula pendula* Roth). The plot was scanned from two positions with a Riegl VZ-2000 scanner (RIEGL Laser Measurement Systems, Horn, Austria). The acquired TLS data were radiometrically calibrated with a Spectralon of a known reflectivity of 99%. Terrain points were removed using the same method as in Section 3.2.1. Leaf and wood points were manually differentiated in the point cloud. Classification results from various methods were available, including laser intensity based, Random Forest machine learning, and an unsupervised segmentation approach in previous studies (Wang et al., 2018). Therefore, this dataset serves as a unique

benchmark to compare our method with other common and state-of-the-art methods. See Wang et al. (2018) for a full description of this dataset and the details on the compared intensity based, Random Forest, and unsupervised segmentation methods.

4. Methods

The proposed pipeline is a concurrent processing routine that operates on a structured superpoint graph. With this representation, an interconnected dual-task processing chain with a series of graph operations is deployed to simultaneously segment graph nodes into clusters (for instance segmentation) and update the contextual information of each node (for semantic embedding) (Fig. 4).

The entire processing routine can be divided into four parts.

- **Geometric partition:** A superpoint is an aggregated representation of a small geometrically simple yet meaningful portion of the point cloud. Therefore, the first step of our method is to partition the point cloud into clusters (i.e., superpoints).
- **Superpoint embedding:** Each superpoint (i.e., graph node) represents a geometrically simple primitive, thus carries a certain degree of semantic information. A fix-size feature vector is inferred for each superpoint.
- **Superpoint graph construction:** A structured and undirected superpoint graph is constructed so that spatially adjacent superpoints are connected by edges (i.e., superedges) (Fig. 5).
- **Graph partition and feature updating:** Superpoint features are updated by the adjacency relationships of the superpoint graph. Nodes in the superpoint graph are segmented into clusters based on superpoint features and the shortest path analysis. Each cluster of superpoint then represents an object instance (i.e., a single tree). Conversely, the path analysis is used to refine and update the semantic information of each superpoint.

We describe in details each step of our pipeline in the following subsections.

4.1. Geometric partition

The aim of this step is not to extract individual objects such as tree branches or leaves. Instead, we seek an over-segmentation to break down the objects into geometrically simple parts. Nevertheless, these simple parts should be semantically homogeneous, so that each part will not contain objects from different classes (Landrieu and Simonovsky, 2018) (Fig. 5).

We deploy a fully automatic graph-based segmentation (Felzenszwalb and Huttenlocher, 2004). The key step is to construct an undirected graph, so that the segmentation is converted to the search of graph connected components. Geometric features (i.e., verticality) and point cloud densities are used to constrain the graph. This segmentation is applied recursively until convergence, so that geometrically and semantically heterogeneous parts are iteratively segmented. Therefore, this data-driven method is adaptive to different data sources and point densities. Details of this segmentation method is referred to Wang et al. (2020).

4.2. Superpoint embedding

Each superpoint \mathcal{S}_i represents a small portion of the entire point cloud. The goal of this step is to independently infer a descriptor for each superpoint by embedding it into a seven-dimensional feature vector $f \in \mathbb{R}$ (Table 1). By doing so, each superpoint carries a degree of semantic information, which will later support the graph partition (Section 4.4).

In addition to several simple features such as size and length, we learn a crucial feature - the initial wood class probability C_p for each

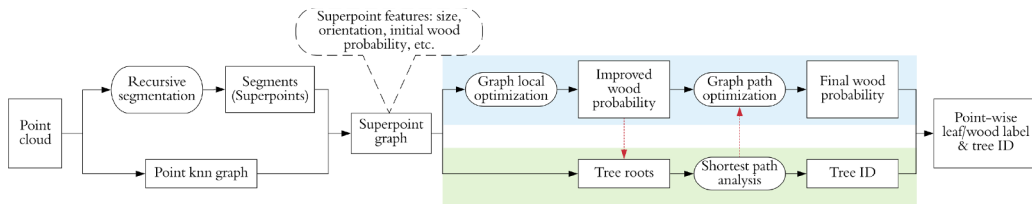


Fig. 4. Workflow of the proposed method. Semantic (i.e., leaf-wood classification, pipeline underlined by blue) and instance (i.e., single tree isolation, pipeline underlined by green) segmentation are conducted simultaneously and collectively. Red arrows indicate mutual benefits of two tasks. (For interpretation of the references to colour in this figure legend, the reader is referred to the web version of this article.)

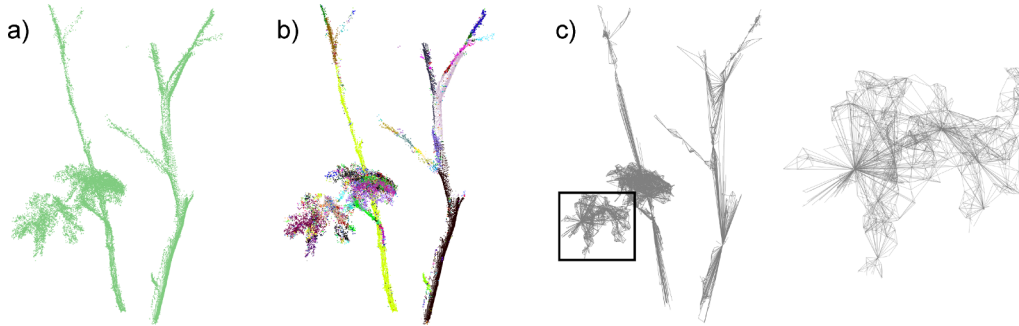


Table 1
List of embedded features f for each superpoint \mathcal{S}_i .

Feature name	Description	Size
Sz	Size, number of points	1
Lp	Lowest point	3
Hp	Highest point	3
L	Length	1
D	Orientation, principle direction	3
Li	Linearity, degree of elongation	1
Cp	Initial wood probability	1

superpoint, since one of the final goals is to classify leaf and wood components. We seek an unsupervised approach, as no prior knowledge on component class is available and required. Wang et al. (2018) showed that wood components can be extracted by identifying linear structures after a point cloud segmentation. First, the linearity Li is calculated from the eigenvalues of the covariance matrix of the superpoint (Wang et al., 2018). Then, by thresholding the size Sz and linearity Li , a superpoint can be labeled as leaf or wood (Wang et al., 2020). However, determinations of these thresholds are not straightforward. Instead, a group of plausible thresholds are tested (Raumonen and Tarvainen, 2018). The outcome is thus a wood class probability known as *soft labeling*. However, this step is still vulnerable to the subjective selection of plausible thresholds. Therefore, we denote this Cp as an initial wood class probability, and it will be further optimized in the following steps.

4.3. Superpoint graph construction

A superpoint graph $\mathcal{G} = (\mathcal{S}, \mathcal{E}, \mathcal{W}, \mathcal{F})$ is consisted of a set of superpoints \mathcal{S} (i.e., nodes), superpoint features $\mathcal{F} \in \mathbb{R}^{|\mathcal{S}| \times f}$, superedges \mathcal{E} , and edge weights $\mathcal{W}: \mathcal{E} \in \mathbb{R}$ mapping the Euclidean distances between superpoints.

To convert a point cloud to a graph, two methods are commonly used. First, a point is connected to its neighbors bounded by either k-nearest neighbors (KNN) or a given radius. Second, point connectivity can be directly modeled by the Delaunay triangulation. In addition, 2D 4-connected or 8-connected graph can be generated if a point cloud projection is available (Ben-Shabat et al., 2018). The graph created

based on neighbors in a given radius is vulnerable to heterogenous point densities, while KNN and Delaunay triangulation based methods may mistakenly connect distant points. Ben-Shabat et al. (2018) compared all these methods on point cloud segmentation, and concluded that KNN should be used if a projection image is not available.

However, a KNN graph cannot be directly constructed over superpoints, because the topology and adjacency relationships are lost for superpoints. In this study, a KNN graph is firstly constructed on the original point cloud, and the connectivity information is then transferred to the superpoints (i.e., superedges) (Fig. 5).

The resulting superpoint graph is a symmetric and undirected graph with embedded superpoints features and superedges representing the adjacency relationships between superpoints.

4.4. Graph partition and feature updating

4.4.1. Graph local optimization

In superpoint embedding, an initial wood class probability Cp is estimated. This initial estimation is applied on individual superpoints, thus lacks contextual information. For example, in practice, the distribution of class labels should be spatially smooth (Landrieu and Simonovsky, 2018). Specifically, most adjacent nodes in the graph would share the same class label. Owing to the rich superpoint features and adjacency relationships, it is possible to directly optimize the initial wood probability in the graph. We use a simple local weighted average approach, which is referred to the graph local optimization in Fig. 4. The initial wood probability Cp of a superpoint is updated by the average value of all Cp of its N neighboring superpoints in the graph (Fig. 6), and is weighted by the size Sz as:

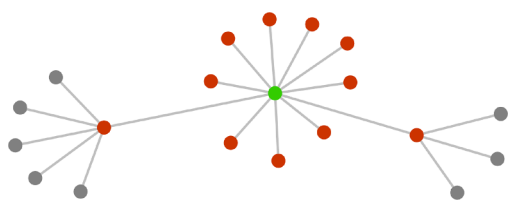


Fig. 6. A superpoint (green) is connected to its neighboring superpoints (red) by superedges. (For interpretation of the references to colour in this figure legend, the reader is referred to the web version of this article.)

$$Cp' = \frac{\sum_{i=1}^N S_{Z_i} Cp_i}{\sum_{i=1}^N S_{Z_i}}. \quad (1)$$

The refined class probability Cp' is denoted as the improved wood probability in Fig. 4. The superpoint graph is thus updated to $\mathcal{G} = (\mathcal{S}, \mathcal{E}, \mathcal{W}, \mathcal{F}')$, with spatially smoothed wood class probabilities in \mathcal{F}' .

4.4.2. Graph shortest path analysis

A path between two superpoints resembles the conducting tubes for transferring water and other nutrients (Tao et al., 2015). For those superpoints representing tree roots (or bases), the paths connect them to other superpoints thus serve as all possible transferring cubes. Based on ecological rules, the conducting path should be the one that maximizes the efficiency (i.e., minimize the traveling distance). Therefore, if multiple instances (i.e., trees) exist in the graph, it is possible to partition the graph by comparing the path distances of superpoints to respective root superpoints. This strategy to isolate individual trees was named comparative shortest path (CSP) in Tao et al. (2015).

The CSP method requires the graph nodes representing single tree bases to be identified first. Previous methods detected tree stems in the original point cloud with Euclidean clustering or circle/cylinder detection methods (e.g., Hackenberg et al., 2015; Burt et al., 2019). While in our method, tree bases can be directly identified by examining the semantic information embedded in superpoint feature sets \mathcal{F}' . First, we remove leaf superpoints whose Cp' are smaller than 0.5. This step has already greatly eliminated the impacts from low vegetation and foliages. Next, tree stem superpoints can be identified by thresholding the geometric features such as size, orientation, and lowest point in Table 1. These stem superpoints are denoted as root superpoints \mathcal{S}_{rt} .

In some cases, detected root superpoints need to be further merged, as multiple \mathcal{S}_{rt} can come from the same tree stem. If a superpoint \mathcal{S}_{rtj} is right above another one \mathcal{S}_{rti} and they have similar orientations, they are likely from the same tree stem (Xia et al., 2015) (Fig. 7). We start from the lowest superpoint, and search for other superpoints above and whose lowest points Lp are within a horizontal distance range d_r to the highest point Hp of current superpoint. If such superpoints exist, the lowest qualified superpoint is merged. This procedure is continued until no superpoints can be merged (Fig. 7). It is noted that this merging only affect the identification of root superpoints \mathcal{S}_{rt} , as only the lowest superpoints of each merged groups are marked as final root superpoints. Thus, the superpoint graph itself is not modified.

Next, the path distances between a superpoint \mathcal{S}_i to all root superpoints \mathcal{S}_{rt} are calculated by the Dijkstra's Shortest Path First algorithm

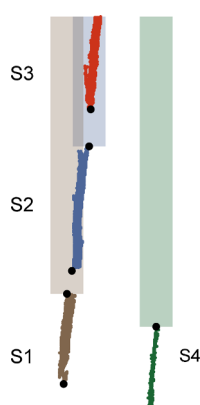


Fig. 7. Iterative merging of root superpoints. \mathcal{S}_1 is firstly merged to \mathcal{S}_1 . Then \mathcal{S}_2 is merged to the new group consisted of \mathcal{S}_1 and \mathcal{S}_2 . The final root superpoints are then \mathcal{S}_1 and \mathcal{S}_4 in this example.

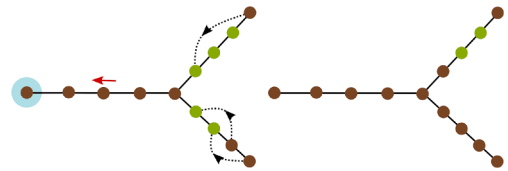


Fig. 8. Graph path optimization for wood detection. Left: a wood superpoint (brown) is retraced to the last leaf superpoint (green) on its path to the root (blue background). Right: the target leaf superpoint is corrected to wood. (For interpretation of the references to colour in this figure legend, the reader is referred to the web version of this article.)

(Dijkstra, 1959). If no paths are available to one or more \mathcal{S}_{rt} , the distances are set to infinite. Each superpoint is clustered to the \mathcal{S}_{rt} that has the shortest path distance. Consequently, each superpoint is clustered to a distinct object instance, determined by respective root \mathcal{S}_{rt} . The superpoint graph is thus partitioned into instances, so that each instance contains superpoints from an individual tree (i.e., a tree ID is added to the feature set \mathcal{F}').

4.4.3. Graph path optimization

The shortest path between a wood superpoint and its root resembles the transferring cube for water and other nutrients. Therefore, the path itself can be used to refine wood detection, as only wood superpoints can act as transferring cubes (Vicari et al., 2019). Specifically, any superpoints on the shortest path from a wood superpoint to its root should be wood as well. Based on this assumption, a retracing and gap filling method was applied in Vicari et al. (2019). We here use a similar approach, by redistributing wood superpoints along the shortest paths towards the roots (Fig. 8). A wood superpoint is retraced to the last leaf superpoints, if exist, on its path. The Cp' of this leaf superpoint is then updated to 0.51 (i.e., wood probability > 0.5). This step is traversed for each wood superpoints. Instead of filling all gaps once (Vicari et al., 2019), this less aggressive strategy avoids the risk that leaf superpoints on the extremities are mistakenly retrieved as well. This step is referred to the graph path optimization (Fig. 4). Consequently, the $\mathcal{G} = (\mathcal{S}, \mathcal{E}, \mathcal{W}, \mathcal{F}')$ is further updated to $\mathcal{G} = (\mathcal{S}, \mathcal{E}, \mathcal{W}, \mathcal{F}'')$, with final wood probabilities Cp'' in \mathcal{F}'' .

4.5. Point-wise labels

The superpoints \mathcal{S} and the feature set \mathcal{F}'' are transformed back to the single point level. The tree ID is directly recorded for each point. A point is labeled as wood if its Cp'' is greater than 0.5, and vice versa.

4.6. Method comparisons

We respectively compared our method with state-of-the-art approaches on single tree isolation and leaf-wood classification. Since previous single tree isolation methods were evaluated on tree stem locating only, thus the comparison here is also on stem locating. The stem detection method in Zhang et al. (2019) was compared on the benchmark datasets described in Section 3.2.1. For leaf-wood classification, multiple methods were compared, including laser intensity, machine learning, and an unsupervised segmentation approach. The benchmark data described in Section 3.2.2 were used for this comparison.

4.7. Assessment

We evaluated the effectiveness of our method on three aspects: (a) detailed crown segmentation, (b) single tree locating, and (c) leaf-wood classification.

4.7.1. Crown segmentation

The assessment of detailed crown segmentation was further divided

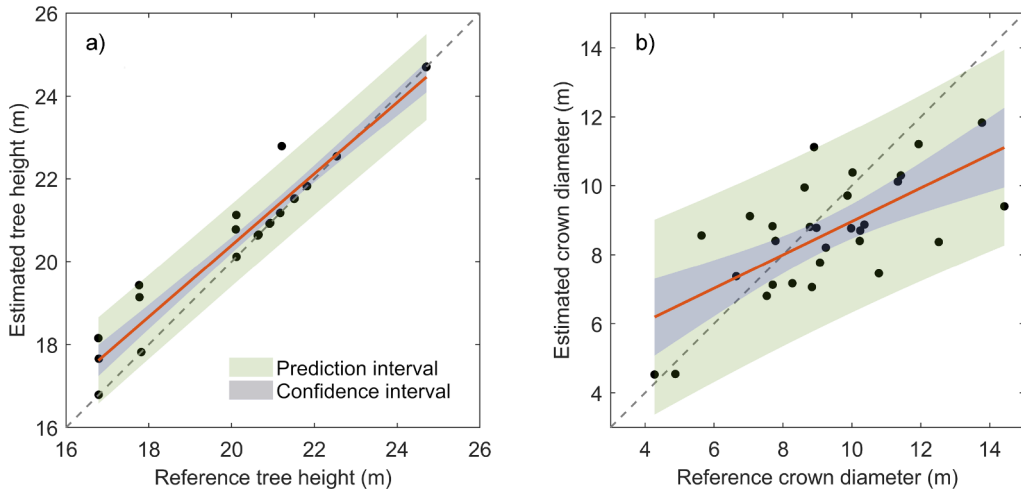


Fig. 9. Assessments of a) tree height and b) crown diameter estimations.

into two parts. First, we used the Intersection over Union (IoU), a standard metric for segmentation evaluation measure, to assess the results of our method on detailed crown segmentation. For an $N \times N$ confusion matrix ($N = 30$ in this study), each entry c_{ij} refers to the number of points from reference tree i predicted as tree j . Then the IoU of tree i is calculated as:

$$\text{IoU}_i = \frac{c_{ii}}{c_{ii} + \sum_{j \neq i} c_{ij} + \sum_{k \neq i} c_{ki}}. \quad (2)$$

The mean IoU (mIoU) of all trees is then estimated by:

$$\text{mIoU} = \frac{\sum_{i=1}^N \text{IoU}_i}{N}. \quad (3)$$

In addition, we also reported the overall accuracy (OA) given by:

$$\text{OA} = 100\% \times \frac{\sum_{i=1}^N c_{ii}}{\sum_{j=1}^N \sum_{k=1}^N c_{jk}}. \quad (4)$$

Second, we additionally evaluated the impacts of crown segmentation on tree height and crown diameter estimations. The root mean square error (RMSE) and its relative value were reported as:

$$\text{RMSE} = \sqrt{\frac{1}{k} \sum_{i=1}^k (y_i - \hat{y}_i)^2}, \quad (5)$$

$$\text{RMSE}(\%) = 100\% \times \frac{\text{RMSE}}{\bar{y}}, \quad (6)$$

where where k is the number of observation data, \hat{y} denotes the reference value and \bar{y} is the mean value of the variable.

4.7.2. Single tree locating

We assessed the results of single tree locating on the benchmark dataset using the metrics of completeness, the correctness, and the mean accuracy of detection, to be consistent with Zhang et al. (2019) and the TLS benchmarking project (Liang et al., 2018). The completeness measures the percentage of detected reference trees. The correctness measures the percentage of detected trees against references. The mean accuracy is the joint metric based on the completeness and correctness, given by:

$$\text{Completeness} = \frac{n_{\text{match}}}{n_{\text{ref}}}, \quad (7)$$

$$\text{Correctness} = \frac{n_{\text{match}}}{n_{\text{extr}}}, \quad (8)$$

$$\text{Mean accuracy} = \frac{2n_{\text{match}}}{(n_{\text{ref}} + n_{\text{extr}})}, \quad (9)$$

where n_{match} is the number of detected reference trees, n_{ref} is the number of reference trees, and n_{extr} is the number of detected trees.

4.7.3. Leaf-wood classification

The same OA metric (Eq. 4) was reported for leaf-wood classification. This metric was used to measure the capability of our method on differentiating leaf and wood components. In addition, the model sensitivity and specificity were reported for leaf-wood classification. Sensitivity measures the true positive (i.e., wood) rate, and specificity gives the true negative (i.e., leaf) rate, given by:

$$\text{Sensitivity} = \frac{\text{TP}}{\text{TP} + \text{FN}}, \quad (10)$$

$$\text{Specificity} = \frac{\text{TN}}{\text{TN} + \text{FP}}, \quad (11)$$

where TP represents true positive and TN the true negative. FP and FN stand for false positive (type I error) and false negative (type II error), respectively.

5. Results

5.1. Synthetic dataset

For detailed crown segmentation, the mIoU was 0.81, with individual IoUs ranging from 0.45 to 1.00. The full confusion matrix can be seen in the [supplementary material](#). The OA was 81.8%. Compared with references, tree height and crown diameter estimations showed a RMSE of 0.01 m (2.9%) and 1.8 m (19.8%), respectively (Fig. 9). The R^2 of the linear regression line (Fig. 9a orange line) for tree height estimation was 0.94, with a slope of 0.86. Nevertheless, the R^2 of the linear regression line (Fig. 9b orange line) for crown diameter estimation was much lower at 0.46. The slope was 0.48, which indicates that the results significantly underestimated crown diameters, especially for large trees. A visualization of crown segmentation is shown in Fig. 10.

On the other hand, our study showed an overall classification accuracy of 87.7%, with a sensitivity of 95.2% and a specificity of 66.8%, for leaf-wood classification. The low specificity means that a large portion of wood points were mistakenly classified as leaf.

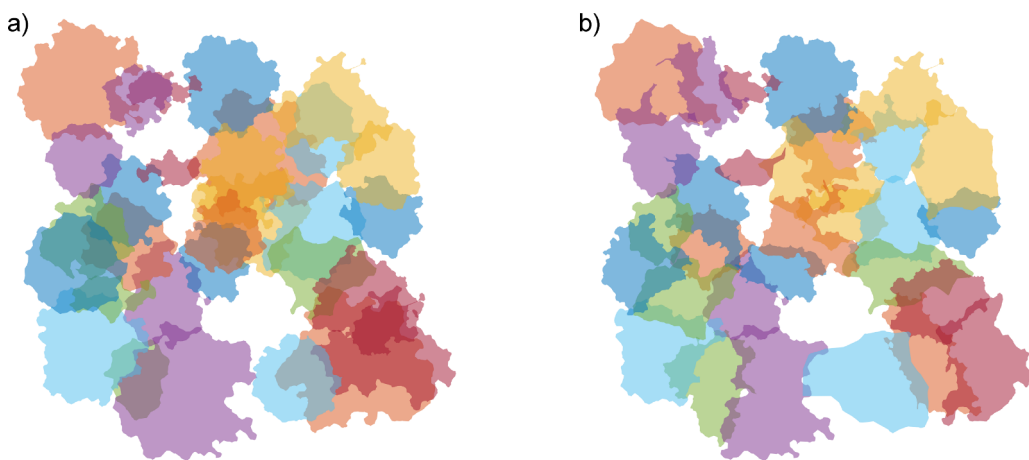


Fig. 10. Crown outlines of a) reference and b) segmented trees.

5.2. Benchmark datasets

5.2.1. Single tree isolation

We additionally evaluated the effectiveness of our study on single tree locating by comparing the results with those from the approach proposed in Zhang et al. (2019), on benchmark datasets of six plots with different complexities. The results were summarized in Table 2. Our method showed much higher completeness, especially for difficult plots. However, the correctness was constantly lower. Overall, our study had higher mean accuracies compared to Zhang et al. (2019).

5.2.2. Leaf-wood classification

The comparisons on leaf-wood classification showed that our method achieved state-of-the-art results, with 88.8% overall accuracy (Table 3). The specificity was generally low for all methods, excepted the Random Forest machine learning approach. Although the sensitivity of our method was marginally lower than that of Wang et al. (2018), whereas the higher specificity balanced the overall accuracy.

5.3. Impacts of TLS scan positions

In practice, the number of TLS scans affects the point cloud density and quality. For forest applications, multiple scans setup is favored because it provides denser point clouds and may avoid occlusions inside tree canopies by acquiring data from different view positions (Liang et al., 2018). However, the ideal point cloud density and spatial coverage cannot be always guaranteed in practice, especially in forests with extremely complex terrain conditions. Therefore, to assess the impacts of TLS scans on our method, we additionally tested the proposed method on the synthetic TLS data acquired from reduced scans with 2, 4 and 5 positions, and compared the respective results with

Table 2

Comparisons between our method and Zhang et al. (2019) on single tree locating of the TLS benchmark dataset. Last row corresponds to mean values.

Plot Complexity	Completeness (%)		Correctness (%)		Mean Accuracy (%)	
	Zhang et al. (2019)	Ours	Zhang et al. (2019)	Ours	Zhang et al. (2019)	Ours
Easy	86.3	90.2	97.8	95.8	91.7	92.9
Easy	82.1	92.9	95.8	81.3	88.5	86.7
Medium	61.5	79.1	100.0	72.2	76.2	75.5
Medium	57.7	78.2	97.8	70.1	72.6	74.0
Difficult	45.8	64.1	93.8	67.2	61.5	65.6
Difficult	26.3	52.5	98.4	70.9	41.5	60.3
	59.9	76.2	97.3	76.3	72.0	75.8

Table 3

Comparisons between our method and others on leaf-wood classification.

	Intensity	Random Forest	Wang et al. (2018)	Ours
Sensitivity (%)	92.1	84.7	96.4	94.3
Specificity (%)	83.1	87.9	81.1	83.3
Overall accuracy (%)	87.6	86.3	88.7	88.8

those from the full 9 scans. Data from 2 scans were obtained from the north and south view points, while 4 scans were from outside the forest (Fig. 3). The scan from the center was further added for data from 5 scans.

Results showed that the number of TLS scans mainly impacted tree height and crown diameter estimations, whereas the accuracy of leaf-wood classification remained stable (Table 4). With reduced TLS scans, the effectiveness of our method for estimating tree height and crown diameter decreased. This implies that our method is more sensitive to tree isolation. The number of TLS scans theoretically determines the degree of occlusions in data at the canopies. If a portion of the canopies is missing or the data are largely fragmented with heterogenous densities, our graph-based method can be problematic as it constructs a graph based on neighborhood cues.

5.4. Algorithm implementation and efficiency

The proposed framework was implemented as an open-source Matlab tool (The MathWorks, Inc., Natick, MA, USA), and is available from the following github repository: <https://github.com/dwang520/SSSC>. We additionally provide a standalone executable that does not require a Matlab to be installed on the user's machine. Tests on algorithm efficiency showed that in average, the processing time was 64 s for 1 million points on a laptop. The processing time had a linear relationship with the total number of points (Fig. 11). The laptop we used to run the algorithm had the following specifications: Windows 10, Intel®Core™ i7-8850H and 32 GB RAM.

6. Discussion

6.1. Joint segmentation with superpoint graphs

Proper understanding of the information content of forest point clouds is curial for subsequent applications. From the perspective of point cloud processing, single tree isolation and leaf-wood classification are two different processes, known as instance and semantic segmentation. The former refers to the process that groups spatially adjacent points into object instances, while the latter is inherently a binary

Table 4

Results from different number of TLS scans for the synthetic dataset.

Number of TLS scans	Tree height	Crown diameter	Leaf-wood classification		
	RMSE	RMSE	Accuracy(%)	Sensitivity(%)	Specificity(%)
9	0.01 m (2.9%)	1.8 m (19.8%)	87.7	95.2	66.8
5	1.5 m (7.3%)	2.8 m (30.4%)	88.4	97.0	69.6
4	1.2 m (6.0%)	3.28 m (35.6%)	88.2	96.6	73.7
2	2.6 m (12.8%)	4.35 m (48.0%)	87.8	96.8	72.1

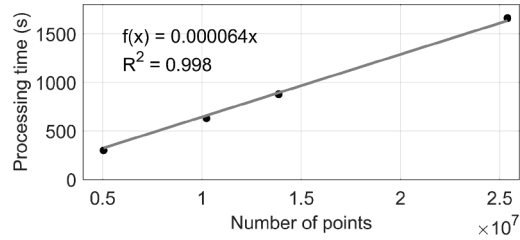


Fig. 11. The relationship between the runtime of our method with point cloud size.

classification problem aiming at identifying a class label to single points. These two problems are fundamental steps for tree-scale quantification using point clouds.

Previous methods tackled these steps as two independent processes. However, we observed that these two steps can be mutually dependent. For example, semantic information on leaf-wood components can assist stem locating by eliminating the interferences from low vegetation and foliages. Therefore, it is desirable to combine semantic and instance segmentation into a single task for forest scenes.

The same desire has been tackled by recent advancements of deep learning networks for computer vision problems (Pham et al., 2019). In such a strategy, each point is firstly learned with a semantic class. Then, points are clustered based on high-dimensional vectors embedded from the semantic class. Finally, the class label and instance indices are regularized by a multi-value conditional random field model. The outcomes are individual objects with semantical class labels. Such advancements indicate that semantic and instance segmentation can be combined with mutual benefits. However, this strategy cannot fulfill our objective, as in computer vision problems, an instance would have a unique class label. In our study, an instance is a single tree and has different class labels in it. Therefore, different strategies are required.

We tackled this problem by using superpoint based graph processing. Instead of direct point cloud manipulation, the inherent "tree" structure of forests makes it possible to leverage graph based processing techniques. Graph based approaches have been previously developed for forest studies separately, including single tree isolation (Tao et al.,

2015), refinement of leaf-wood classification (Vicari et al., 2019), and tree skeleton extractions (Du et al., 2019). These studies indicated a potential of using graph based approaches to integrate tree isolation and components classification. However, this potential remains unexplored.

We linked these steps with a superpoint graph, and showed that each step could complement each other with joint graph optimizations. In addition, there are two distinct advantages of using superpoint graph for large scale point cloud processing. First, it operates on the object level instead of individual points. The number of objects (i.e., superpoints) is typically several order of magnitude smaller than the number of points (Landrieu and Simonovsky, 2018). This enables us to efficiently process large scale datasets. Second, objects contain feature information that single points lack (Wang et al., 2018). It is possible to semantically describe each object and the relationships between adjacent objects, which is very useful for the leaf-wood classification task.

6.2. Instance segmentation - single tree isolation

Single tree isolation involves two critical steps - single tree locating and crown segmentation. For TLS point clouds, single tree locating is usually referring to tree stem extraction and crown segmentation is regarded as a subsequent process following stem locating. Our study used the similar algorithm of comparative shortest path algorithm in Tao et al. (2015). Nevertheless, our method directly identifies tree stems in the graph, benefiting from the embedded rich superpoint features.

One of the obstacles of evaluating a single tree isolation method is the lack of reference data on crowns. Therefore, previous methods assessed their performances on stem locating only, except Heinzel and Huber (2018). The assessment of crown segmentation was done visually, or often ignored. In this study, the synthetic TLS data simulated from a highly realistic scene enable us to assess detailed crown segmentation. The mIoU of 0.81 implies that crowns were generally well segmented. A visual inspection in Fig. 12 indicates that problems occurred inside those heavily intersected crowns. Especially when crowns were deeply overlapped, the shortest path analysis failed. It is noted that the simulation in this study was purely statistical, and did not

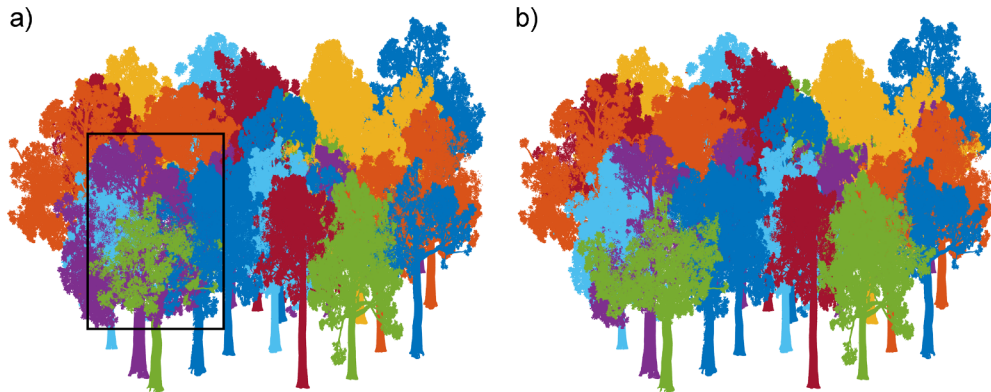


Fig. 12. Single tree isolation. a) Reference. b) Our result. Each tree is colored randomly. The black rectangle in a) indicates a challenging region to segment.

consider the ecological basis. For example, tree crowns will unlikely intersect significantly in practice, due to growth competitions for sun-lights (Thorpe et al., 2010). Nevertheless, our method showed promising results for trees having well defined crown boundaries (Fig. 10 and 12). The assessments of tree height and crown diameters also demonstrated that our method can be effectively used for crown level metrics retrieval (Fig. 9).

Despite the advantages of synthetic datasets for having explicit references for crown segmentation, the deficiencies are obvious. Forest scene components such as terrain, understory, and other vegetation elements including mosses and lianas are difficult to model. Therefore, their impacts on the TLS data quality and the methodology were ignored. Notably, the potential negative impacts such as occlusions cannot be neglected for tree stem locating, which is the crucial step prior to crown segmentation.

To address this problem, we further included a benchmark dataset to assess the effectiveness of our method for locating single tree stems. This openly available dataset was from an international endeavor on TLS approaches for forest inventories (Liang et al., 2018), thus allows us to easily compare the results. Results showed that our method achieved much higher completeness comparing to a recent study of Zhang et al. (2019), meaning that more trees were identified by our method (Table 2). This is particularly notable for difficult plots, for which the completeness was more than 59% from our method, whereas Zhang et al. (2019) had 36%. However, the correctness was lower in this study. A low correctness metric implies that many identified stems are not in the reference. We further diagnosed this issue visually. An example is given in Fig. 13, in which all detected stems were inspected in a difficult plot. We observed that most detected stems were indeed tree stems. Our method detected stems of small trees and shrubs that were not included in the reference, which resulted the low correctness. The trees that were not detected by our method were mainly distributed at the edge of the plot, a region where a low point cloud density was expected. Nonetheless, we achieved a higher mean accuracy compared to Zhang et al. (2019) for single tree locating.

6.3. Semantic segmentation - leaf-wood classification

We tested the proposed method on a synthetic and a benchmark dataset for leaf-wood classification. The synthetic dataset contained trees with heavily intersected crowns. The crowns had large sizes and complex shapes. These factors led to heavy occlusions and a challenging condition for acquiring high quality TLS data.

The results on the synthetic dataset showed an overall accuracy of 87.7%, which is similar to other studies (e.g., Ma et al., 2015; Zhu et al.,

2018; Wang et al., 2018; Vicari et al., 2019). However, the model specificity was rather low at 66.8%, meaning that many wood points were lost in the classification. Visual inspection revealed that the classification difficulty occurred mainly inside tree crowns (Fig. 14). Small and thin branches were difficult to detect. Our method detected linear structures, thus can be problematic if those small branches were fragmented in point clouds.

Point cloud quality is one of the main prerequisites for successful leaf-wood classification (Vicari et al., 2019). In the synthetic data, impacts from TLS scanning setups, co-registration, understory occlusions, and winds were neglected. These factors are difficult to include in the simulation. Therefore, the low model specificity was mainly attributed to the occlusions inside tree crowns. To further evaluate the effectiveness of our method on leaf-wood classification, we included an additional benchmark from a real forest in Austria. Comparisons with other studies showed that our method achieved the highest overall accuracy (Table 3). The comparison also revealed a systematic trend that unsupervised methods tend to have lower model specificity than sensitivity. Conversely, the Random Forest machine learning approach had higher specificity, indicating its effectiveness in detecting wood points. Machine learning approaches often look at geometric features from the neighborhood of each point, implying that local density might be a particular useful feature in identifying wood points. Unsupervised methods thus can be potentially improved by incorporating such information, such as by using post-processing spherical filters around each point (e.g., Ma et al., 2015; Vicari et al., 2019).

In our pipeline, the leaf-wood classification was firstly estimated during the superpoint embedding. Then, two optimization steps were applied, one using graph adjacency relationships, and another one using path information after the instance segmentation. The results showed that the overall accuracy was improved from 79.6% to 87.7% for the synthetic dataset, and from 84.7% to 88.8% for the benchmark dataset, with these optimizations. The local optimization was aiming at improving the spatial homogeneity of class labels, as adjacent points would share the same class label. The adjacency relationships were inherently embedded in the graph, making our method naturally suitable for graph-based optimization, which is a standard technique for label smoothing (Li et al., 2019). The path optimization was mainly used to improve the specificity by retrieving wood points, based on the assumption that only wood points can serve as transferring tubes for water and nutrients on the path from/to tree roots. Approximately 1% improvement on the specificity was achieved for both datasets with the path optimization. Overall, our study proved that single tree isolation and leaf-wood classification can be conducted simultaneously, and can indeed complement each other.

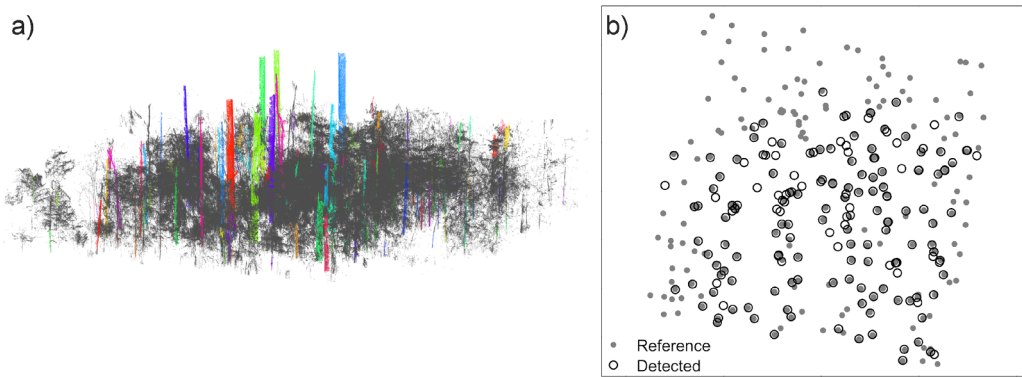


Fig. 13. Stem locating of a difficult plot in the benchmark dataset. a) Each identified stem is colored randomly. Other low non-stem points (i.e., below 5 m above ground) are colored by gray. b) Comparison between reference stem locations and our result.

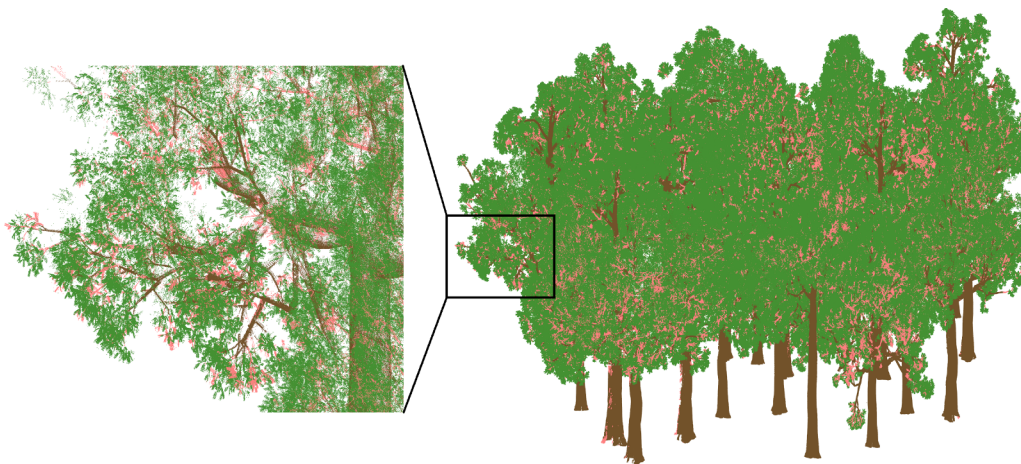


Fig. 14. Leaf-wood classification result of the synthetic plot. Green and brown color stand for correctly classified leaf and wood points. Pink refers to wrongly classified points. The magnified view on the left corresponds to the black rectangle area. (For interpretation of the references to colour in this figure legend, the reader is referred to the web version of this article.)

7. Conclusion

Semantic and instance segmentation of forest point clouds are crucial and fundamental steps in tree-scale analysis. In this study, we presented an unsupervised pipeline that simultaneously performs single tree isolation and leaf-wood classification. The proposed method was based on a novel superpoint graph embedded with rich node and edge features. A joint dual-task network enabled the learning of class labels and clustering of points with graph operators.

We evaluated the proposed method on a synthetic TLS dataset simulated on a highly realistic forest plot. For the first time, single tree isolation was evaluated on detailed crown segmentation. We also compared the proposed method with existing methods on other benchmark datasets. Results showed that we achieved state-of-the-art performances on both single tree locating and leaf-wood classification tasks.

The proposed method provides a significant advance in TLS and forest applications. We demonstrated that the prerequisite of interpreting the information content of forest point clouds can be achieved effectively and fully automatically. In addition, we provide the proposed method as an open-source tool with an end-user interface, and it is our hope that it can be used by the TLS and forestry research communities to facilitate certain data processing chains.

Declaration of Competing Interest

The authors declare that they have no known competing financial interests or personal relationships that could have appeared to influence the work reported in this paper.

Acknowledgments

This study was supported by a postdoctoral fellowship of the School of Engineering, Aalto University.

Appendix A. Supplementary material

Supplementary data associated with this article can be found, in the online version, at <https://doi.org/10.1016/j.isprsjprs.2020.04.020>.

References

- Barbeito, I., Dassot, M., Bayer, D., Collet, C., Drössler, L., Löf, M., Del Rio, M., Ruiz-Peinado, R., Forrester, D.I., Bravo-Oviedo, A., et al., 2017. Terrestrial laser scanning reveals differences in crown structure of *fagus sylvatica* in mixed vs. pure European forests. *For. Ecol. Manage.* **405**, 381–390.
- Bechtold, S., Höfle, B., 2016. HELIOS: A multi-purpose lidar simulation framework for research, planning and training of lidar scanning operations with airborne, ground-
- based mobile and stationary platforms. *ISPRS Ann. Photogramm., Remote Sens. Spatial Informat. Sci.* III-3, 161–168. <https://doi.org/10.5194/isprs-annals-III-3-161-2016>.
- Béland, M., Baldocchi, D.D., Widlowski, J.L., Fournier, R.A., Verstraete, M.M., 2014. On seeing the wood from the leaves and the role of voxel size in determining leaf area distribution of forests with terrestrial lidar. *Agric. For. Meteorol.* **184**, 82–97.
- Belton, D., Moncrieff, S., Chapman, J., 2013. Processing tree point clouds using gaussian mixture models. In: Proceedings of the ISPRS Annals of the Photogrammetry, Remote Sensing and Spatial Information Sciences, Antalya, Turkey, pp. 11–13.
- Ben-Shabat, Y., Avraham, T., Lindenbaum, M., Fischer, A., 2018. Graph based over-segmentation methods for 3d point clouds. *Comput. Vis. Image Underst.* **174**, 12–23.
- Burt, A., Disney, M., Calders, K., 2019. Extracting individual trees from lidar point clouds using treeseg. *Methods Ecol. Evol.* **10**, 438–445.
- Calders, K., Disney, M.I., Armston, J., Burt, A., Brede, B., Origo, N., Muir, J., Nightingale, J., 2017. Evaluation of the range accuracy and the radiometric calibration of multiple terrestrial laser scanning instruments for data interoperability. *IEEE Trans. Geosci. Remote Sens.* **55**, 2716–2724.
- Calders, K., Newnham, G., Burt, A., Murphy, S., Raumonen, P., Herold, M., Culvenor, D., Avitabile, V., Disney, M., Armston, J., et al., 2015. Nondestructive estimates of above-ground biomass using terrestrial laser scanning. *Methods Ecol. Evol.* **6**, 198–208.
- Danson, F.M., Hetherington, D., Morsdorf, F., Koetz, B., Allgower, B., 2007. Forest canopy gap fraction from terrestrial laser scanning. *IEEE Geosci. Remote Sens. Lett.* **4**, 157–160.
- Dassot, M., Constant, T., Fournier, M., 2011. The use of terrestrial lidar technology in forest science: application fields, benefits and challenges. *Ann. For. Sci.* **68**, 959–974.
- Dijkstra, E.W., 1959. A note on two problems in connexion with graphs. *Numerische Mathematik* **1**, 269–271.
- Disney, M., 2019. Terrestrial lidar: a three-dimensional revolution in how we look at trees. *New Phytol.* **222**, 1736–1741.
- Disney, M.I., Boni Vicari, M., Burt, A., Calders, K., Lewis, S.L., Raumonen, P., Wilkes, P., 2018. Weighing trees with lasers: advances, challenges and opportunities. *Interface Focus* **8**, 20170048.
- Du, S., Lindenbergh, R., Ledoux, H., Stoter, J., Nan, L., 2019. Adtree: Accurate, detailed, and automatic modelling of laser-scanned trees. *Remote Sensing* **11**.
- Felzenszwalb, P.F., Huttenlocher, D.P., 2004. Efficient graph-based image segmentation. *Int. J. Comput. Vision* **59**, 167–181.
- Gastellu-Etchegorry, J.P., Yin, T., Lauret, N., Cajigfinger, T., Gregoire, T., Grau, E., Feret, J.B., Lopes, M., Guilleux, J., Dedieu, G., et al., 2015. Discrete anisotropic radiative transfer (dart 5) for modeling airborne and satellite spectroradiometer and lidar acquisitions of natural and urban landscapes. *Remote Sensing* **7**, 1667–1701.
- Hackenberg, J., Specker, H., Calders, K., Disney, M., Raumonen, P., 2015. Simpletree—an efficient open source tool to build tree models from tls clouds. *Forests* **6**, 4245–4294.
- Heinzel, J., Huber, M., 2018. Constrained spectral clustering of individual trees in dense forest using terrestrial laser scanning data. *Remote Sensing* **10**, 1056.
- Hétroy-Wheeler, F., Casella, E., Boltcheva, D., 2016. Segmentation of tree seedling point clouds into elementary units. *Int. J. Remote Sens.* **37**, 2881–2907.
- Kaasalainen, S., Krooks, A., Kukko, A., Kaartinen, H., 2009. Radiometric calibration of terrestrial laser scanners with external reference targets. *Remote Sensing* **1**, 144–158.
- Krishna Moorthy, S.M., Calders, K., Vicari, M.B., Verbeeck, H., 2019. Improved supervised learning-based approach for leaf and wood classification from lidar point clouds of forests. *IEEE Trans. Geosci. Remote Sens.* **1**, 1–14.
- Landrieu, L., Simonovsky, M., 2018. Large-scale point cloud semantic segmentation with superpoint graphs. In: Proceedings of the IEEE Conference on Computer Vision and Pattern Recognition, pp. 4558–4567.
- Li, N., Liu, C., Pfeifer, N., 2019. Improving lidar classification accuracy by contextual label smoothing in post-processing. *ISPRS J. Photogramm. Remote Sens.* **148**, 13–31.
- Li, S., Dai, L., Wang, H., Wang, Y., He, Z., Lin, S., 2017. Estimating leaf area density of individual trees using the point cloud segmentation of terrestrial lidar data and a voxel-based model. *Remote Sensing* **9**, 1202.
- Liang, X., Hyppä, J., Kaartinen, H., Lehtomäki, M., Pyörälä, J., Pfeifer, N., Holopainen, M., Broly, G., Francesco, P., Hackenberg, J., et al., 2018. International benchmarking of terrestrial lidar scanning approaches for forest inventories. *ISPRS J. Photogramm.*

- Remote Sens. 144, 137–179.
- Liang, X., Kankare, V., Hyppä, J., Wang, Y., Kukko, A., Haggrén, H., Yu, X., Kaartinen, H., Jaakkola, A., Guan, F., et al., 2016. Terrestrial laser scanning in forest inventories. *ISPRS J. Photogramm. Remote Sens.* 115, 63–77.
- Liu, J., Wang, T., Skidmore, A.K., Jones, S., Heurich, M., Beudert, B., Premier, J., 2019. Comparison of terrestrial lidar and digital hemispherical photography for estimating leaf angle distribution in European broadleaf beech forests. *ISPRS J. Photogramm. Remote Sens.* 158, 76–89.
- Ma, L., Zheng, G., Eitel, J.U., Moskal, L.M., He, W., Huang, H., 2015. Improved salient feature-based approach for automatically separating photosynthetic and non-photosynthetic components within terrestrial lidar point cloud data of forest canopies. *IEEE Trans. Geosci. Remote Sens.* 54, 679–696.
- Momo Takoudjou, S., Ploton, P., Sonké, B., Hackenberg, J., Griffon, S., De Coligny, F., Kamdem, N.G., Libalah, M., Mofack, G.I., Le Moguédec, G., et al., 2018. Using terrestrial laser scanning data to estimate large tropical trees biomass and calibrate allometric models: A comparison with traditional destructive approach. *Methods Ecol. Evol.* 9, 905–916.
- Morsdorf, F., Kükenbrink, D., Schneider, F.D., Abegg, M., Schaeppman, M.E., 2018. Close-range laser scanning in forests: towards physically based semantics across scales. *Interface Focus* 8, 20170046.
- Moudrý, V., Klápsič, P., Fogl, M., Gdulová, K., Barták, V., Urban, R., 2020. Assessment of lidar ground filtering algorithms for determining ground surface of non-natural terrain overgrown with forest and steppe vegetation. *Measurement* 150, 107047.
- Pham, Q.H., Nguyen, D.T., Hua, B.S., Roig, G., Yeung, S.K., 2019. JSIS3D: Joint semantic-instance segmentation of 3d point clouds with multi-task pointwise networks and multi-value conditional random fields. In: Proceedings of the IEEE Conference on Computer Vision and Pattern Recognition (CVPR).
- Puttonen, E., Krooks, A., Kaartinen, H., Kaasalainen, S., 2014. Ground level determination in forested environment with utilization of a scanner-centered terrestrial laser scanning configuration. *IEEE Geosci. Remote Sens. Lett.* 12, 616–620.
- Raumonen, P., Casella, E., Calders, K., Murphy, S., Åkerblom, M., Kaasalainen, M., 2015. Massive-scale tree modelling from tis data. *ISPRS Ann. Photogramm., Remote Sens. Spatial Inf. Sci.* II-3/W4, 189–196.
- Raumonen, P., Tarvainen, T., 2018. Segmentation of vessel structures from photoacoustic images with reliability assessment. *Biomed. Opt. Exp.* 9, 2887–2904.
- Gonzalez de Tanago, J., Lau, A., Bartholomeus, H., Herold, M., Avitabile, V., Raunonen, P., Martius, C., Goodman, R.C., Disney, M., Manuri, S., et al., 2018. Estimation of above-ground biomass of large tropical trees with terrestrial lidar. *Methods Ecol. Evol.* 9, 223–234.
- Tao, S., Guo, Q., Xu, S., Su, Y., Li, Y., Wu, F., 2015. A geometric method for wood-leaf separation using terrestrial and simulated lidar data. *Photogramm. Eng. Remote Sens.* 81, 767–776.
- Tchapmi, L., Choy, C., Armeni, I., Gwak, J., Savarese, S., 2017. Segcloud: Semantic segmentation of 3d point clouds. In: 2017 International Conference on 3D Vision (3DV), IEEE, pp. 537–547.
- Thorpe, H.C., Astrup, R., Trowbridge, A., Coates, K.D., 2010. Competition and tree crowns: a neighborhood analysis of three boreal tree species. *For. Ecol. Manage.* 259, 1586–1596.
- Trochta, J., Krusek, M., Vrška, T., Král, K., 2017. 3d forest: An application for descriptions of three-dimensional forest structures using terrestrial lidar. *PLOS One* 12, 1–17.
- Van Leeuwen, M., Coops, N.C., Hilker, T., Wulder, M.A., Newnham, G.J., Culvenor, D.S., 2013. Automated reconstruction of tree and canopy structure for modeling the internal canopy radiation regime. *Remote Sens. Environ.* 136, 286–300.
- Vicari, M.B., Disney, M., Wilkes, P., Burt, A., Calders, K., Woodgate, W., 2019. Leaf and wood classification framework for terrestrial lidar point clouds. *Methods Ecol. Evol.* 10, 680–694.
- Wang, D., Brunner, J., Ma, Z., Lu, H., Hollaus, M., Pang, Y., Pfeifer, N., 2018. Separating tree photosynthetic and non-photosynthetic components from point cloud data using dynamic segment merging. *Forests* 9, 252.
- Wang, D., Hollaus, M., Puttonen, E., Pfeifer, N., 2016. Automatic and self-adaptive stem reconstruction in landslide-affected forests. *Remote Sens.* 8, 974.
- Wang, D., Momo Takoudjou, S., Casella, E., 2020. Lewos: A universal leaf-wood classification method to facilitate the 3d modelling of large tropical trees using terrestrial lidar. *Methods Ecol. Evol.* 11, 376–389.
- Wang, J., Chen, X., Cao, L., An, F., Chen, B., Xue, L., Yun, T., 2019. Individual rubber tree segmentation based on ground-based lidar data and faster r-cnn of deep learning. *Forests* 10, 793.
- West, G.B., Brown, J.H., Enquist, B.J., 1997. A general model for the origin of allometric scaling laws in biology. *Science* 276, 122–126.
- Wilkes, P., Lau, A., Disney, M., Calders, K., Burt, A., de Tanago, J.G., Bartholomeus, H., Brede, B., Herold, M., 2017. Data acquisition considerations for terrestrial laser scanning of forest plots. *Remote Sens. Environ.* 196, 140–153.
- Xia, S., Wang, C., Pan, F., Xi, X., Zeng, H., Liu, H., 2015. Detecting stems in dense and homogeneous forest using single-scan tls. *Forests* 6, 3923–3945.
- Yang, B., Dai, W., Dong, Z., Liu, Y., 2016. Automatic forest mapping at individual tree levels from terrestrial laser scanning point clouds with a hierarchical minimum cut method. *Remote Sensing* 8, 372.
- Yun, T., An, F., Li, W., Sun, Y., Cao, L., Xue, L., 2016. A novel approach for retrieving tree leaf area from ground-based lidar. *Remote Sensing* 8, 942.
- Zhang, W., Qi, J., Wan, P., Wang, H., Xie, D., Wang, X., Yan, G., 2016. An easy-to-use airborne lidar data filtering method based on cloth simulation. *Remote Sensing* 8, 501.
- Zhang, W., Wan, P., Wang, T., Cai, S., Chen, Y., Jin, X., Yan, G., 2019. A novel approach for the detection of standing tree stems from plot-level terrestrial laser scanning data. *Remote Sensing* 11, 211.
- Zhong, L., Cheng, L., Xu, H., Wu, Y., Chen, Y., Li, M., 2016. Segmentation of individual trees from tls and mls data. *IEEE J. Sel. Top. Appl. Earth Obser. Remote Sens.* 10, 774–787.
- Zhu, X., Skidmore, A.K., Darvishzadeh, R., Niemann, K.O., Liu, J., Shi, Y., Wang, T., 2018. Foliar and woody materials discriminated using terrestrial lidar in a mixed natural forest. *Int. J. Appl. Earth Obser. Geoinformat.* 64, 43–50.